Theor Appl Climatol (2016) 126:161–182
DOI 10.1007/s00704-015-1557-0

ORIGINAL PAPER

Regional climate simulations over Vietnam using the WRF model

S. V. Raghavan[1,2,3] · M. T. Vu[1,2,3] · S. Y. Liong[1,2,3]

Received: 5 February 2014 / Accepted: 1 July 2015 / Published online: 28 July 2015

Abstract We present an analysis of the present-day (1961–1990) regional climate simulations over Vietnam. The regional climate model Weather Research and Forecasting (WRF) was driven by the global reanalysis ERA40. The performance of the regional climate model in simulating the observed climate is evaluated with a main focus on precipitation and temperature. The regional climate model was able to reproduce the observed spatial patterns of the climate, although with some biases. The model also performed better in reproducing the extreme precipitation and the interannual variability. Overall, the WRF model was able to simulate the main regional signatures of climate variables, seasonal cycles, and frequency distributions. This study is an evaluation of the present-day climate simulations of a regional climate model at a resolution of 25 km. Given that dynamical downscaling has become common for studying climate change and its impacts, the study highlights that much more improvements in modeling might be necessary to yield realistic simulations of climate at high resolutions before they can be used for impact studies at a local scale. The need for a dense network of observations is also realized as observations at high resolutions are needed when it comes to evaluations and validations of models at sub-regional and local scales.

✉ S. V. Raghavan
tmsvs@nus.edu.sg

1 Tropical Marine Science Institute, National University of Singapore, Singapore, Singapore

2 Center for Environmental Sensing and Modeling, SMART, Singapore, Singapore

3 Center for Hazards Research, Dept. of Civil and Environmental Engineering, National University of Singapore, Singapore, Singapore

1 Introduction

Using general circulation models (GCMs), which are primary tools for the prediction of global climate, the Intergovernmental Panel on Climate Change (IPCC) has estimated the global climate sensitivity (the equilibrium change in global mean surface temperature following a doubling of the atmospheric CO_2 concentration) to be in the range of 2 to 4.5 °C with a best estimate of about 3 °C and is very unlikely to be less than 1.5 °C (IPCC, 2007). The fourth assessment report of the IPCC has stated that increasing temperatures are likely to increase the frequency and severity of weather events such as heat waves and heavy rainfall and could lead to large-scale effects such as melting of large ice sheets, with major impacts on low-lying regions throughout the world (IPCC, 2007). Since these projected climate changes will impact water resources, agriculture, bio-diversity, and health, one of the key challenges of climate research is the application of climate models to quantify future climate change and its impacts on both the physical environment and the society through the employment of impact models (Hewitson and Crane, 2006). Although there is a need to understand the possible impacts of climate change and variability at a global scale, when considering the societal response and its adaptive strategies, the regional impacts and local consequences of large-scale change need to be addressed. It has been noted that the GCMs provide better simulation accuracy of present-day climate in a global, hemispheric, or a continental scale but at a regional scale representation, their simulation accuracies are poor (Giorgi, 1990). Regional and sub-regional climates are often affected by forcings and circulations such as cyclones, mesoscale convective systems, and land/sea breezes that occur at a sub-grid scale of the GCM. The coarse resolution of the GCM makes it unsuitable for undertaking detailed impact studies at regional and sub-regional scales. Importantly, precipitation is one of the most widely used climate variable in several impact studies; however, it is a difficult parameter to be simulated realistically owing to its nature of being highly variable in space and time. This warrants a “downscaling” of large-scale climate using high resolution regional climate models (RCMs) owing to their “added value” in hopefully yielding more realistic climate simulations in space and time than GCMs.

The use of RCMs in climate research has been extensive basically owing to their higher spatial resolutions and their ability to include fine scale topography. They have been used to realistically simulate regional climate features such as orographic precipitation (Frei et al., 2003), extreme climate events (Fowler et al., 2005a; Frei et al., 2006), and regional scale climate anomalies or non-linear effects, such as those associated with the El Niño Southern Oscillation (ENSO) (Leung et al., 2004). Several applications of regional climate models have been discussed at length by Wang et al. (2004). However, the model skill depends strongly on biases inherited from the driving GCM and the presence and strength of regional scale forcings such as orography, land-sea contrast, and vegetation cover. Some research studies within the western USA, Europe, and New Zealand, where topographic effects on temperature and precipitation are prominent, have reported more skill in dynamical downscaling than in regions such the Great Plains of the USA and China where regional forcings are weaker (Wang et al., 2004). It has also been observed that the application of RCMs to geographically diverse regions and model inter-comparison studies have allowed the strengths and weaknesses of dynamical downscaling to be better understood (Wang et al., 2004; Leung et al., 2004). Research studies have noted that dynamical downscaling can also provide improved simulations of mesoscale precipitation processes and thus higher moment climate statistics producing more plausible climate change scenarios for extreme events and climate variability at regional scales (Schmidli et al., 2006).

Similar downscaling studies have also been performed over Southeast Asia and over Vietnam. Chotamonsak et al. (2011) performed regional climate simulations over Southeast Asia using the Weather Research and Forecasting (WRF) (Skamarock et al., 2008) model driven by GCM ECHAM5 under the IPCC A1B emission scenario. Dynamical downscaling of the GCM ECHAM5 was done at a 60-km horizontal resolution to project changes from 1990–1999 to 2045–2054 of temperature and compared against observations. The study reported that when the model simulations were compared against observations, the regional climate model reproduced the spatial distribution of temperature, although with a cold bias for maximum surface temperatures and a warm bias for minimum temperatures. The wet season (rainy) precipitation was simulated with lesser skill than the dry season precipitation. Future changes in precipitation showed increases on an average but with local decreases during the dry season. Takahashi et al. (2009) used the WRF model to assess changes in the September month rainfall over the Indochina peninsula over the period 1966–1995, the WRF model driven by the ERA40 reanalyses. The authors reported that the WRF model successfully simulated the observed long-term decrease in rainfall and concluded that the weakening tropical cyclone activity over the Indochina Peninsula region was the likely reason for the decrease in rainfall. In another study, Takahashi et al. (2010) also performed a control simulation using the WRF model driven by reanalysis data combined with land use and predicted soil moisture data over Indochina. It was reported that the comparison of the control simulations with observations showed that the simulation captured the spatial distribution of the total amount of precipitation over and around the Indochina Peninsula. In addition, the simulated height of the planetary boundary layer and vertical structure of water vapor also corresponded to the observations which indicated that the control simulations reproduced realistic sensible and latent heat fluxes. The regional climate model RegCM3 (Regional Climate Model version 3.0) was used to address the seasonal and interannual variations of rainfall and temperature over Vietnam by Phan et al. (2009), the model being driven by the ERA40 reanalyses. The study reported that the model better reproduced the observed annual cycle and interannual variability of rainfall and temperature and that the simulated patterns of these variables were in good agreement against observed data.

In this paper, the WRF model was employed to simulate the observed climate (precipitation and temperature) of Vietnam.

Vietnam is located in Southeast Asia, bounded between the latitudes of 8 to 23°N and longitudes of 102 to 109°E. The total land area occupies 330,992 km^2. Vietnam has a 1400-km borderline to the North with China, 2067 km with Laos and Cambodia to the West, and has a coast line of 3260 km. Apart from two offshore archipelagos, Hoang Sa (Danang province) and Truong Sa (Khanh Hoa Province), Vietnam also has 3000 big and small islands with total area of more than 1600 km^2. Three fourths of Vietnam’s territory is covered by mountains and hills with the elevation ranging between 100 to 1000 m. Based on topography, Vietnam is divided into seven regions: Northern upland region, Red River Delta, Northern Central Coast, South Central Coast, Central Highland, Northern East of the South, and Mekong Delta. However, in this paper, we have chosen three main regions with regard to their climate zones based on their geographical classification, North, Center, and South, for model evaluations (Fig. 1). Due to differences in latitudes and the distinguished variety of topography, the climate of Vietnam tends to vary considerably from

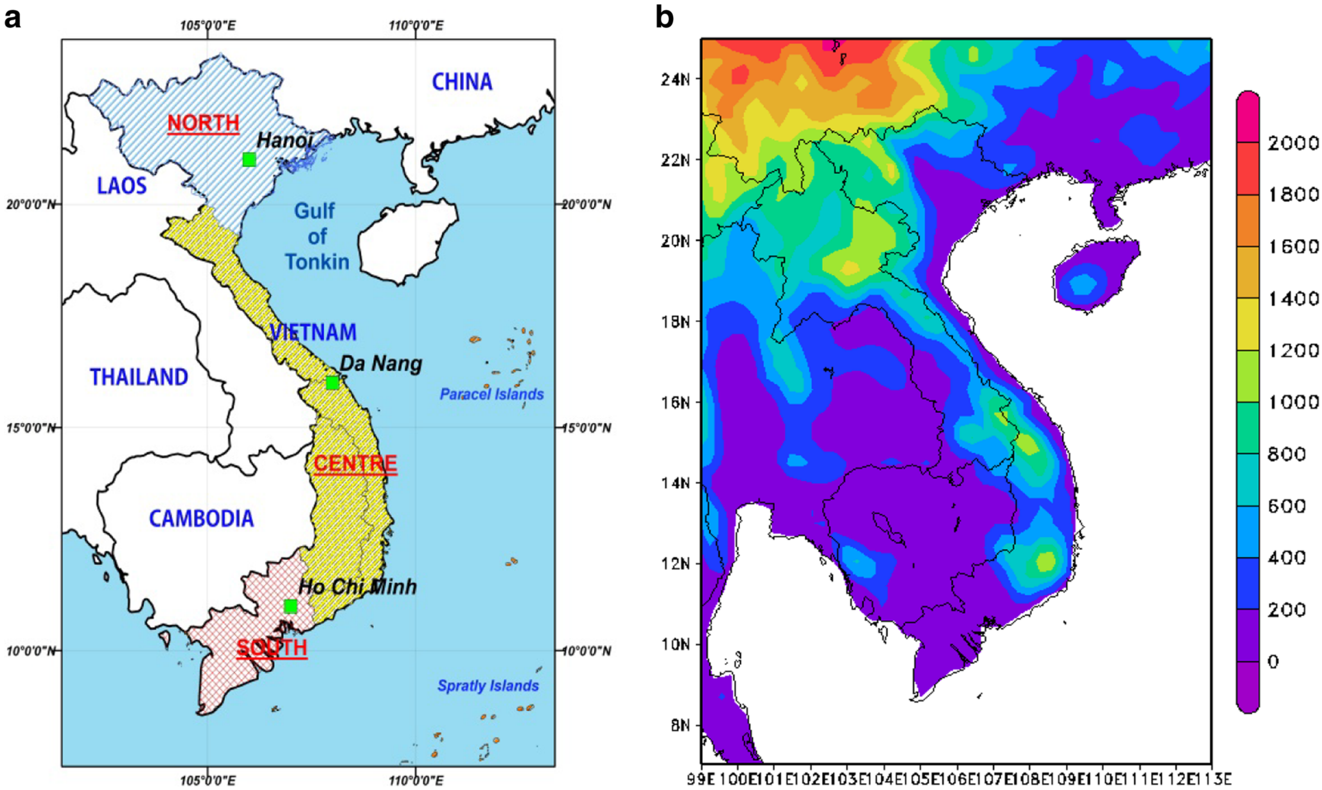

Fig. 1 **a** WRF model domain set-up showing major locations.**b** Topography over the domain

place to place. During the winter or dry season, extending roughly from November to April, the monsoon winds usually blow from the north-east along the China coast and across the Gulf of Tonkin, drawing considerable moisture. Contrastingly, the winter season in most parts of the country is dry when compared to the rainy or summer season (June to September). The average annual temperature is generally higher in the coastal areas than in the mountains and plateaus and in the south than in the north. Temperatures in the southern plains vary less, ranging between 21 and 28 °C during a year. The seasons in the mountains and plateaus and in the north experiencing temperature ranges from 5 °C in December and January to 37 °C in July and August (Source: Mekong River Commission (MRC) report, available at www.mrcmekong.org).

2 Model and data

The regional climate simulations in this study were performed using the WRF model, developed at the National Center for Atmospheric Research (NCAR), USA. The WRF model is basically a mesoscale numerical weather prediction (NWP) system designed to serve both operational forecasting and atmospheric research needs. WRF is suitable for a broad spectrum of applications across scales ranging from meters to thousands of kilometers. WRF uses a three-dimensional grid to represent the atmosphere at scales ranging from meters to thousands of kilometers, topographical land information, and observational data to define initial conditions for a forecasting simulation. The model incorporates advanced numeric and data assimilation techniques, a multiple relocatable nesting capability, and numerous state-of-the-art physics options.

The WRF model used in this study was initialized on 00Z 1 January 1960, and the simulation was continued until the 18Z 31 December 1990. The global reanalysis data ERA-40 (European Reanalysis 40 years) was used to provide the lateral boundary conditions to the WRF model for the period 1961–1990. This data is a global atmospheric analysis of many conventional observations and satellite data streams available over the period September 1957–August 2002 (Uppala et al., 2005). It was developed by the European Centre for Medium Range Weather Forecasts (ECMWF). Analyses were produced daily at 0, 6, 12, and 18 h. The atmospheric model was at a spatial resolution of 40 km run with 60 levels in the vertical, and the output was made available as a gridded data at a spatial resolution of 2.5 × 2.5°.

The first year of the WRF simulations was considered as the spin-up time. The domain configuration with its topography is shown in Fig. 1b. The WRF model was simulated at a 25 × 25 km resolution with 60 grid points on the east-west

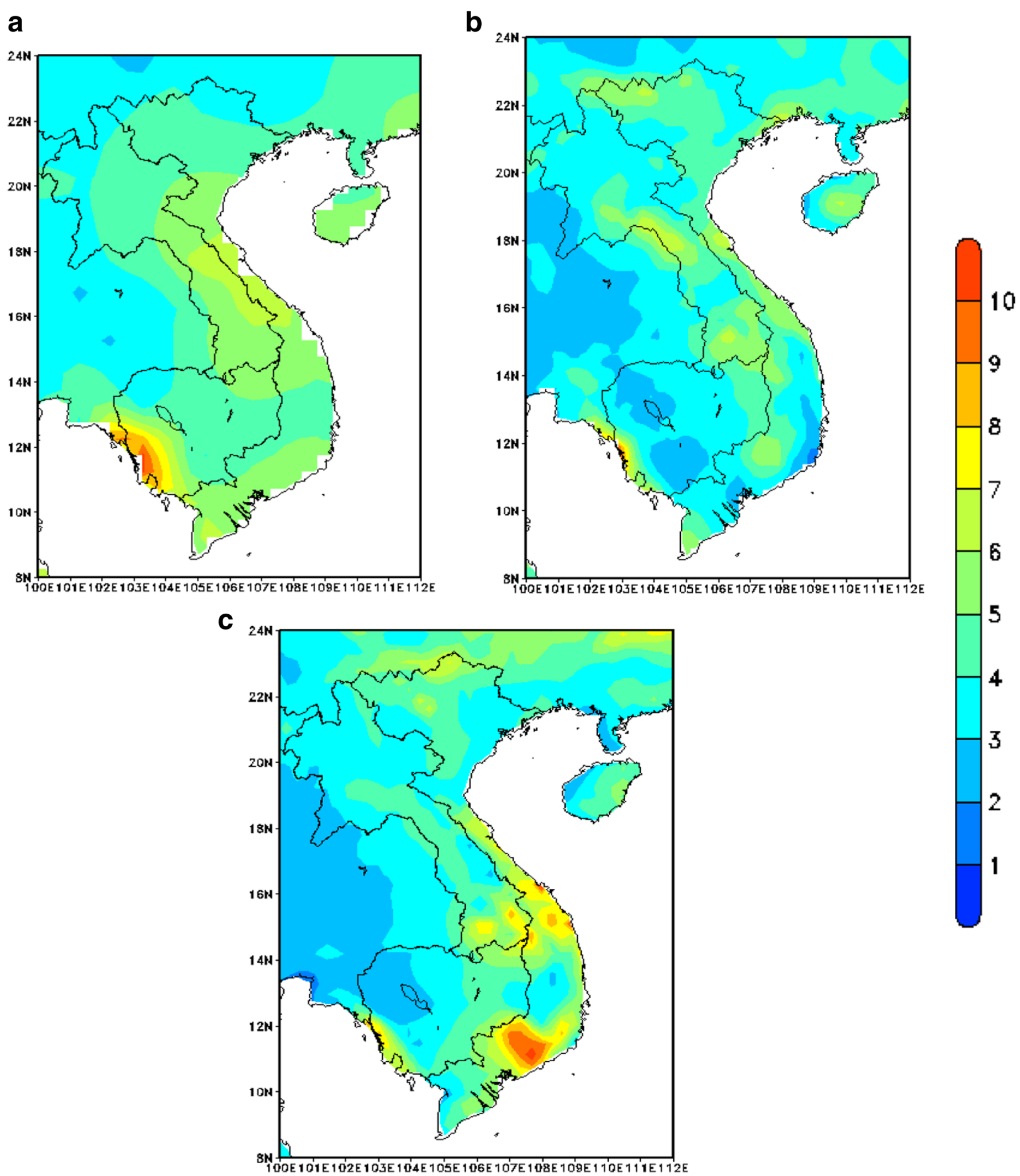

Fig. 2 Mean annual precipitation, mm/day, 1961–1990.**a** CRU, **b** APH, **c** WRF/ERA40

direction and 70 grid points on the north-south, allowing a 10 grid point buffer zone on the lateral boundaries. The physical parameterization used are the Grell cumulus scheme (Grell, 1993), Thomson microphysics scheme (Thompson et al., 2004), Yonsei University planetary boundary layer scheme (Hong and Pan, 1996), rapid radiative transfer model (RRTM), longwave and shortwave radiations, and the four-layer soil moisture and temperature Noah Land Surface model (Chen and Dudhia, 2001).

The WRF model requires initial and time evolving boundary conditions for the climate variables temperature, winds, geopotential height, relative humidity and surface pressure, and sea surface temperature. These variables

Table 1 Areal average annual precipitation for three main regions: North, Center, and South

Mean	North	Center	South
APHRO	4.35	4.18	3.71
CRU	4.34	5.37	5.37
WRF/ERA40	4.21	5.67	5.13

were provided to the WRF model using the ERA40 reanalyses at 6 hourly intervals. Since a land surface component was also in place with the WRF model, additional surface variable soil moisture and temperature for four layers below the ground surface were also provided from the reanalyses as initial conditions.

Two gridded observational datasets were used for model validations for the 1961–1990 period. These are the high

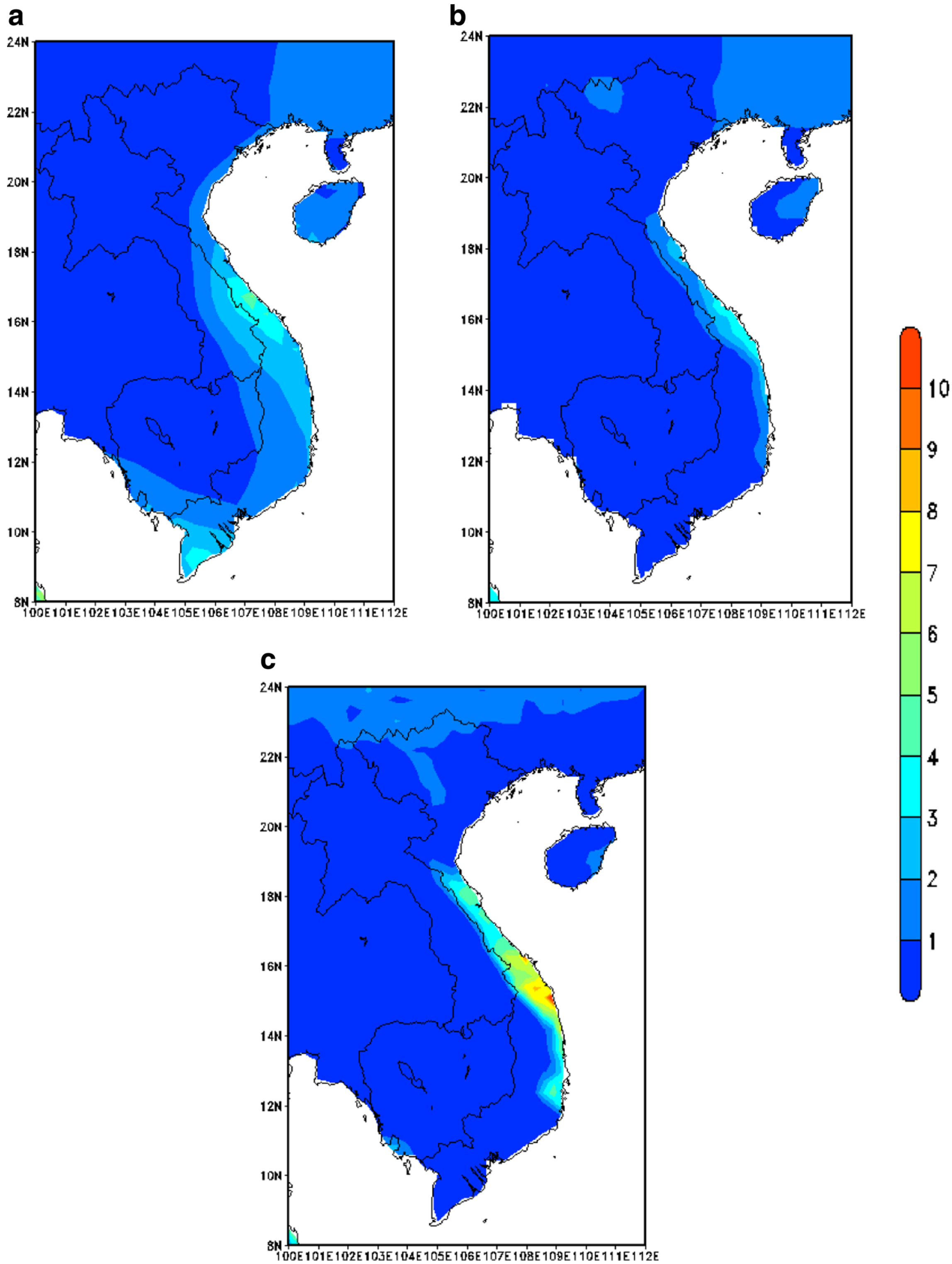

Fig. 3 Mean seasonal precipitation, DJF, 1961–1990, mm/day. **a** CRU, **b** APH, **c** WRF/ERA40

resolution (0.5°) monthly datasets for precipitation and temperature, developed at the Climatic Research Unit (CRU) at the University of East Anglia (New et al., 1999, 2000; Mitchell and Jones (2005)) and the 0.25° daily precipitation dataset APHRODITE, developed by the Research Institute for Humanity and Nature (RIHN) and the Meteorological Research Institute of Japan Meteorological Agency (MRI/JMA), Japan (http://www.chikyu.ac.jp/precip/) (Yatagai et al., 2012). Daily Station data for precipitation and temperature were also obtained from three station locations in Vietnam:

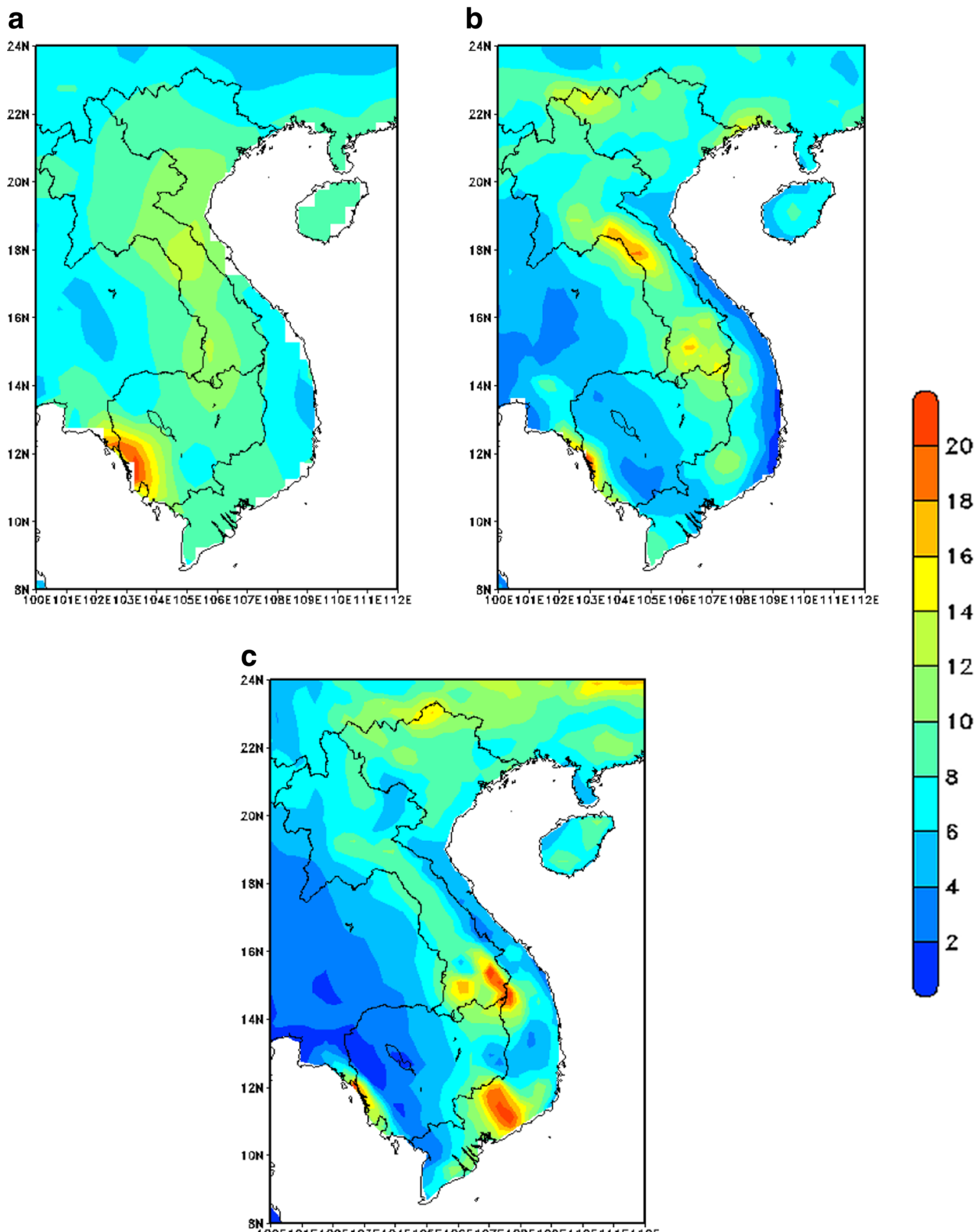

Fig. 4 Mean seasonal precipitation, JJA, mm/day, 1961–1990. **a** CRU, **b** APH, **c** WRF/ERA40

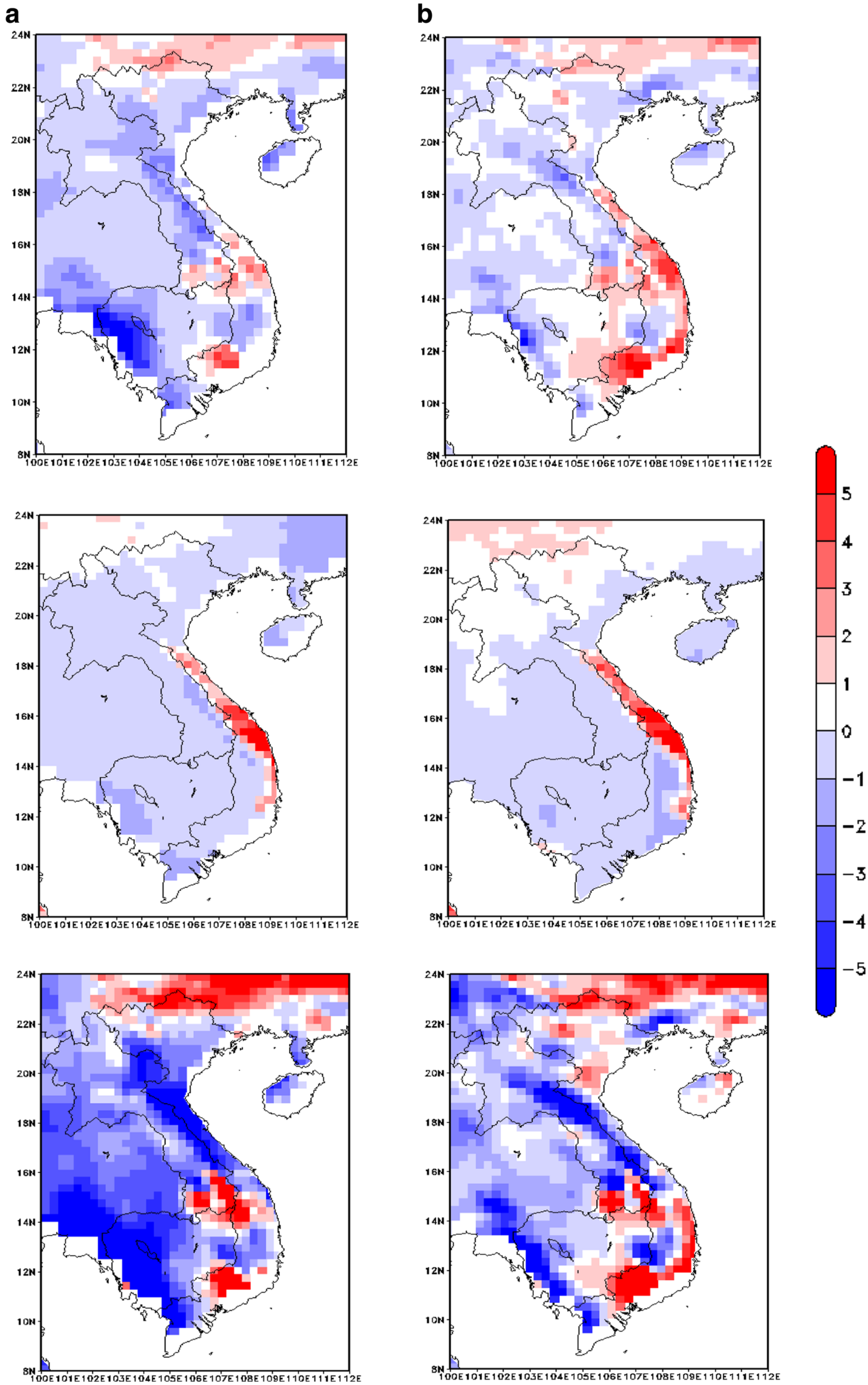

Fig. 5 Bias: WRF/ERA40 minus OBS; mean precipitation, mm/day, 1961–1990. OBS: **a** CRU, **b** APH. Annual (*top*), DJF (*middle*), and JJA (*bottom*)

Hanoi, Danang, and Ho Chi Minh City (each station location representative for each of the three climatic zones that were chosen for this study).

3 Results

To evaluate the WRF model performance, 30-year simulations for the period 1961–1990 are compared against the gridded observational datasets and station data. The model performance is evaluated on annual and seasonal (December–January–February, DJF and June–July–August, JJA) periods for precipitation and temperature and on the seasonal scales alone for the wind fields. Although the domain configuration in the different plotted results includes the Indochina peninsular region, the discussion in this paper is focused only on Vietnam.

The mean annual precipitation for the period 1961–1990 simulated by the WRF model is compared against different gridded observations in Fig. 2. There is a good agreement over the central parts of Vietnam. Over some regions of Northern and Central Vietnam, Laos, and Cambodia, there is a better agreement of the model against APHRODITE data than CRU. The areal averages over different regions also show that the WRF model was able to capture the mean rainfall amounts. The rainfall values of the model and observations are compared in Table 1.

At the outset, it is noticeable that there are considerable uncertainties among the different gridded observations which could be due to the number of stations accounted for and different interpolation methods used in developing these datasets. The multiple observations help to place the model simulations within a range of uncertainties, but a detailed quantification of the observational uncertainties is out of scope of this paper.

The mean seasonal (DJF and JJA) precipitation patterns are shown in Figs. 3 and 4, respectively. The winter season DJF precipitation shows very good agreement against the gridded observations. During the summer season, JJA, there is good agreement over parts of northern and central Vietnam, but lesser precipitation is evident over the Mekong Delta region. Much of the whole domain in simulation shows higher precipitation, and this suggests that some improvement in model simulations is necessary during the summer time. Among the observations, the APHRODITE shows general drier precipitation distributions than CRU.

The WRF model also exhibits some dry bias (Fig. 5) over some regions of Northern Vietnam and over the Mekong Delta region. The annual and seasonal biases in precipitation are shown in Fig. 5a–c. The WRF model exhibits a dry mean annual bias of about 1–2 mm over Northern Vietnam; higher positive biases are seen over the Central regions. Overall, there are least biases in the WRF model when compared to APHRODITE data. The winter time biases are seen in some central regions which could be due to precipitation over the mountainous regions, where there are no observations. The model simulates orographic rainfall over these mountains not accounted for in the gridded observations (due to lack of gauges at remote sites), and this gives rise to the biases seen in the figure. The summer time biases are larger, especially over the western regions of Vietnam.

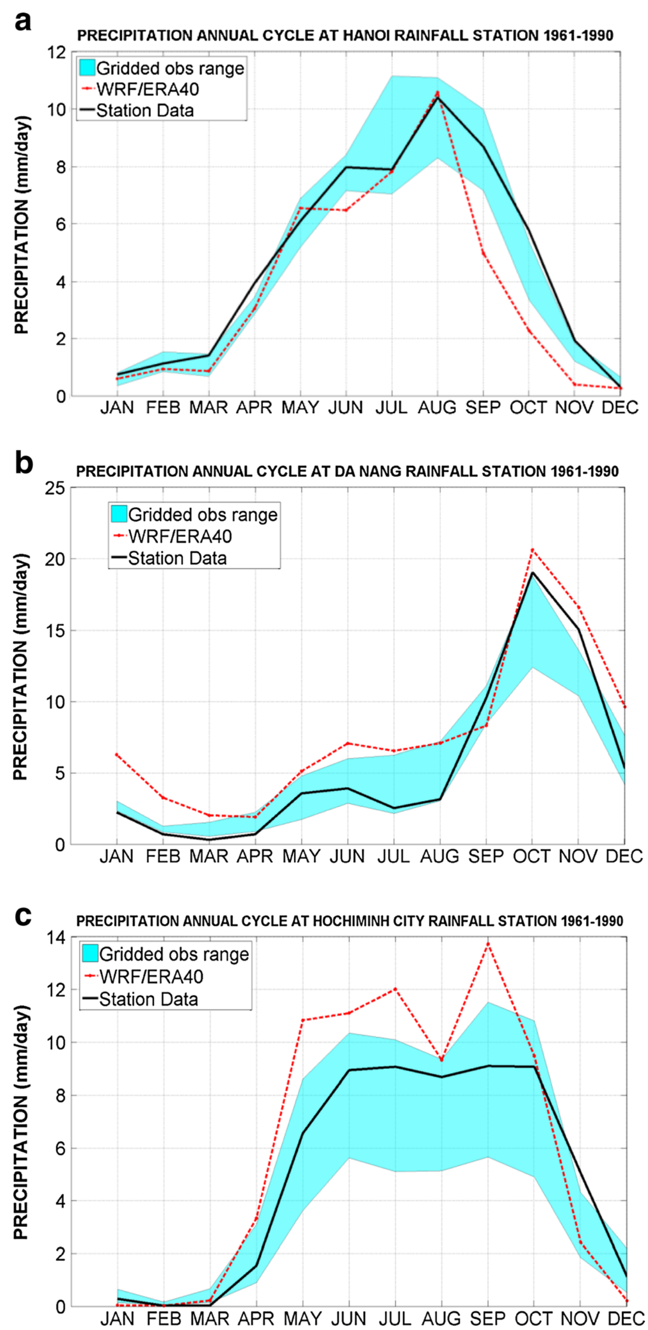

Fig. 6 Mean annual cycle of precipitation, mm/day, 1961–1990. **a** Hanoi, **b** Da Nang, **c** Ho Chi Minh City

The mean annual cycles of precipitation for the three stations, Hanoi, Danang, and Ho Chi Minh City are shown in Fig. 6. The different gridded observations have been shown as a band in the figure to represent the wide range of observed

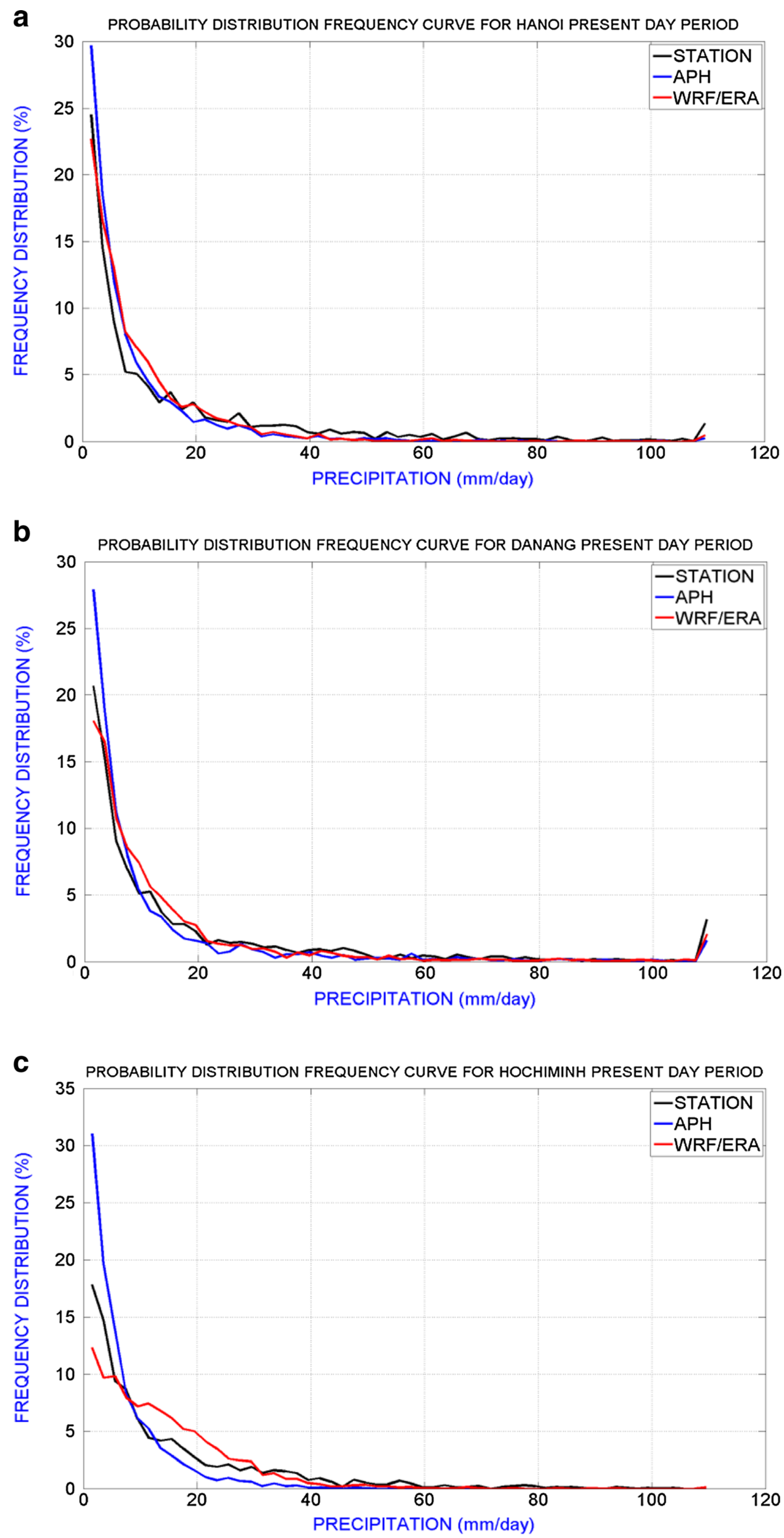

Fig. 7 Probability density function of rainfall, mm/day, 1961–1990. **a** Hanoi, **b** Da Nang, **c** Ho Chi Minh City

uncertainties, while the station data and the WRF model-derived precipitation are shown as curves. The WRF model was able to resolve the overall signatures of the annual cycles. For the Hanoi station, the WRF model closely follows the station data until September when a deficit exists through to December. For Danang station, the model shows a good agreement in the signature of the seasonal cycles, except overestimating the mean monthly rainfall over the most of the months. This could be due to the overestimation seen in the spatial distributions of precipitation over the central regions during the summer months. For Ho Chi Minh City, WRF model overestimates precipitation, especially during the summer months and also exhibits a pronounced double peak in the annual cycle which is less pronounced in the station data.

It is imperative to evaluate the model on its ability to resolve extremes, something which has profound implications when the model is used for studying future climate projections. To this end, the probability density functions (PDFs) for the three station locations, bi-linearly interpolated and derived from the WRF model, are compared to the station data in Fig. 7. The daily APHRODITE data is also plotted along with

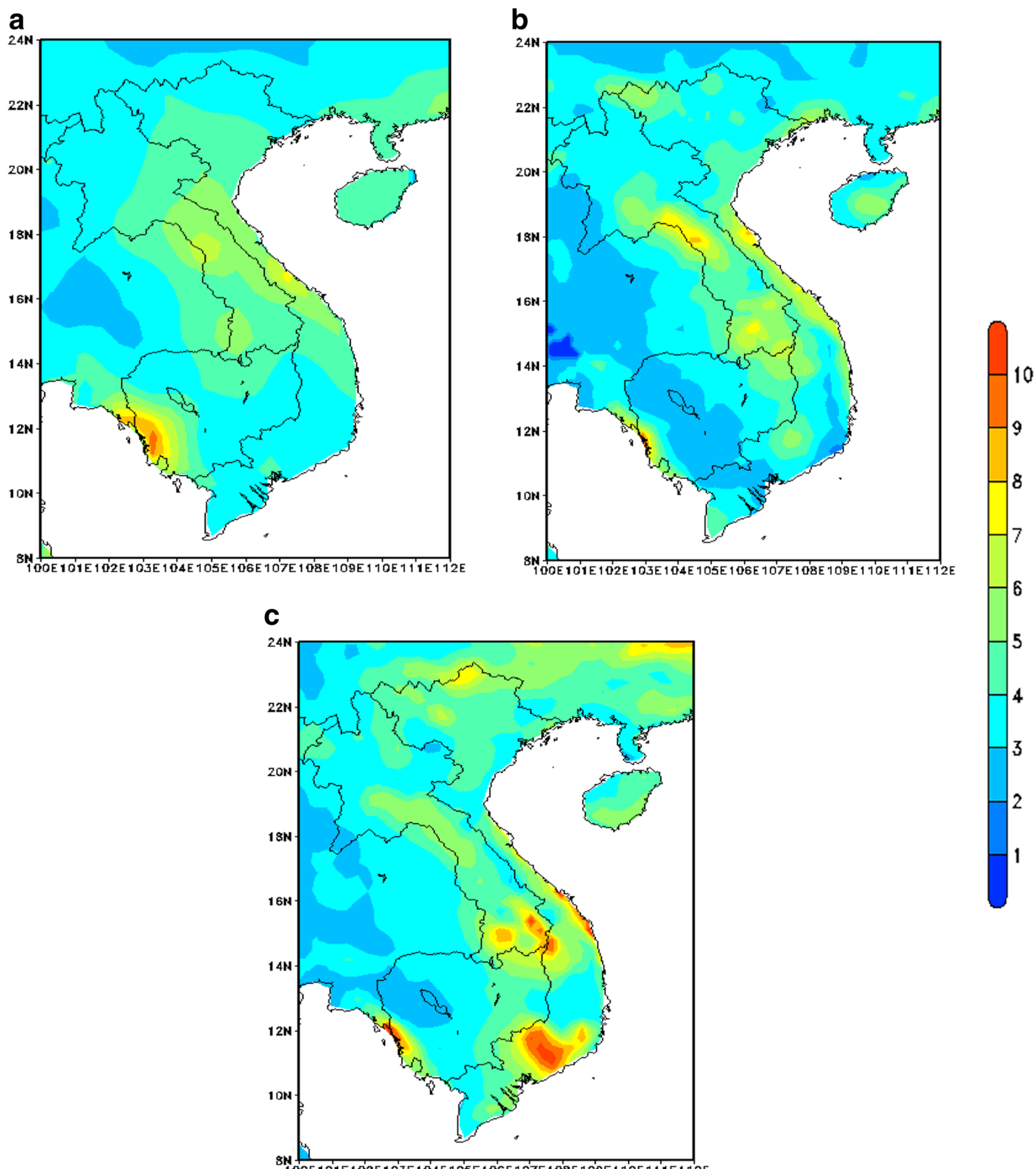

Fig. 8 Root mean square anomaly of mean annual rainfall, mm/day, 1961–1990. **a** CRU, **b** APH, **c** WRF/ERA40

station and model data. The WRF model shows a good agreement of rainfall intensities against observations over Hanoi and Da Nang than Ho Chu Minh city, however, is unable to reproduce the dry days. The high rain intensity days are better resolved for all the three stations. Overall, the PDFs suggest that the model was able to simulate rainfall intensities and extremes to a fairly good extent as we compare a point (station) location against a model (25 km box)-derived data.

It is also important for the model to reproduce the interannual variability for the present-day period 1961–1990. This is shown in Fig. 8, as the root mean square anomaly or the interannual standard deviation of the precipitation. The WRF model exhibits good performance of this variability over most of the Vietnam region when compared to CRU. However, the variability is slightly higher than in all other observations. Larger variability is seen in the APHRODITE data, which is

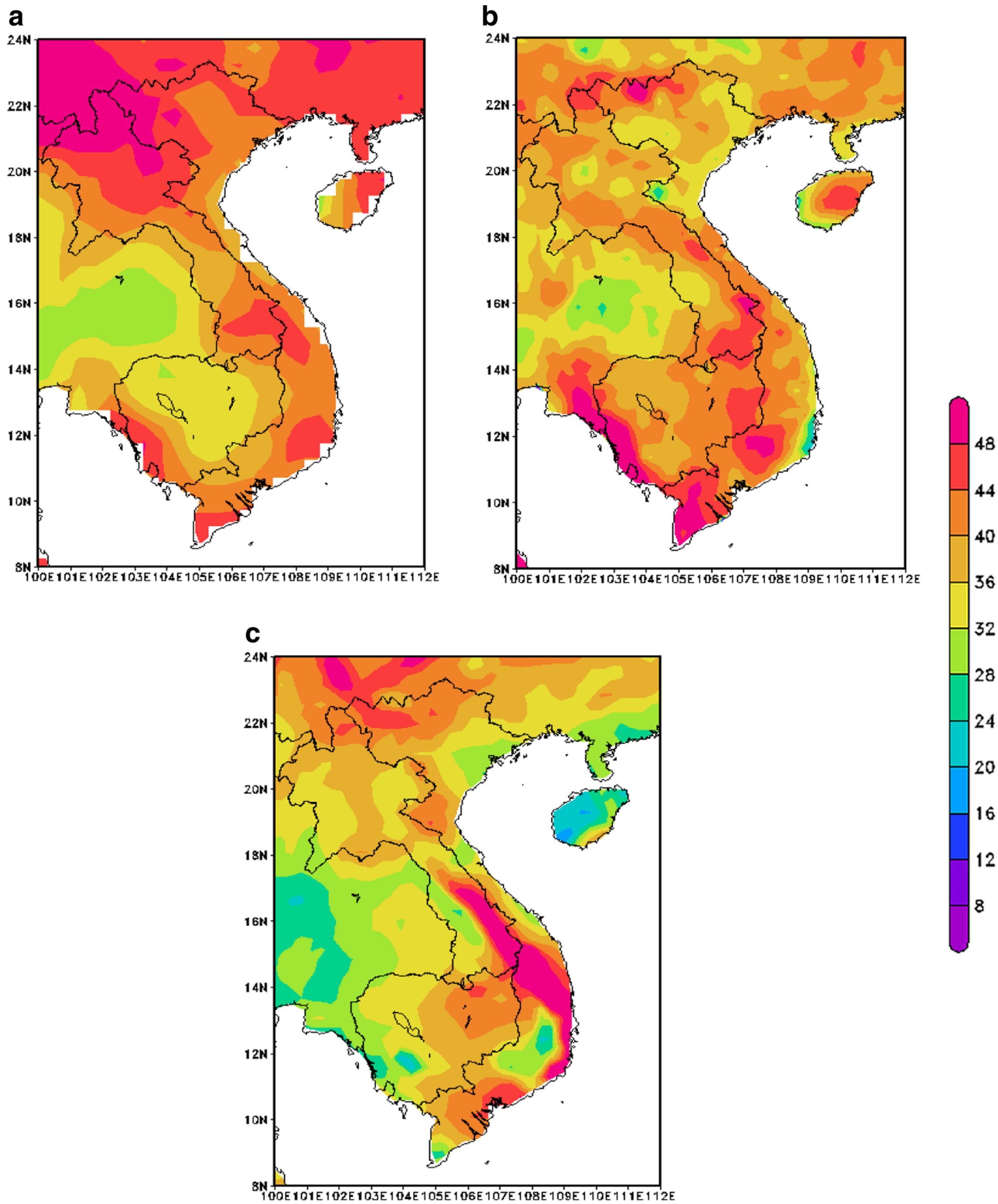

Fig. 9 Annual number of wet days (%), 1961–1990. **a** CRU, **b** APH, **c** WRF/ERA40

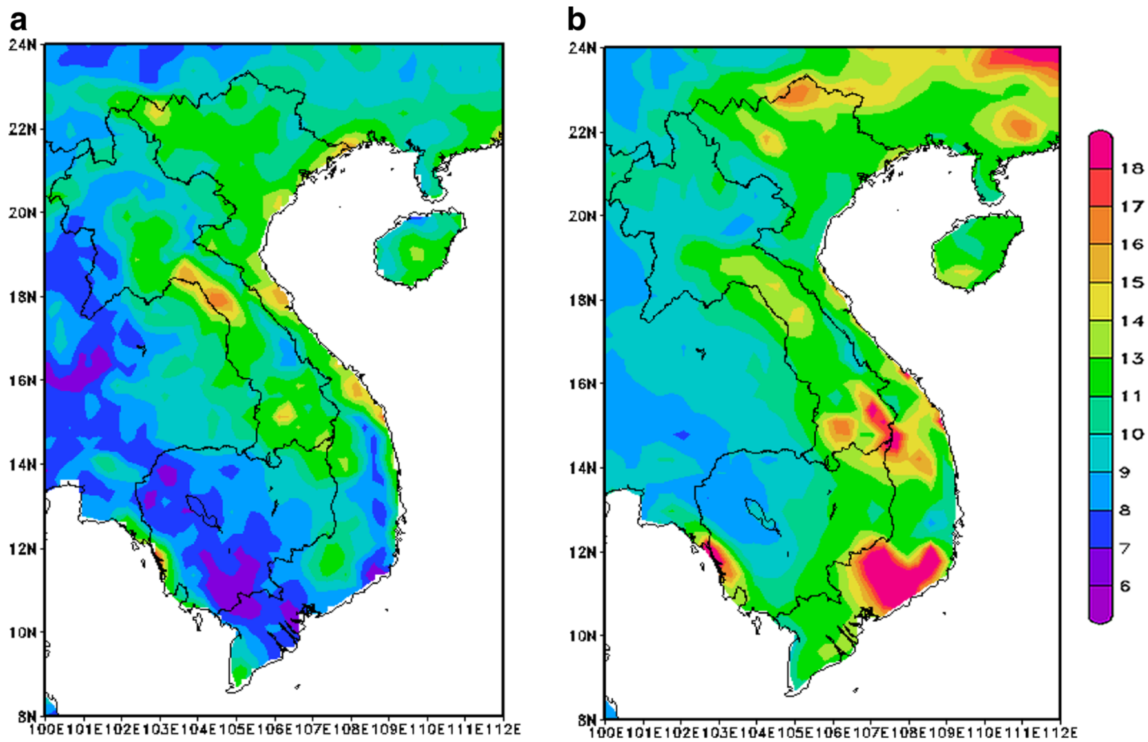

Fig. 10 Annual simple daily intensity index, mm/day, 1961–1990. **a** APH, **b** WRF/ERA40

on daily time scale. The model also exhibits higher variations of differences over the eastern coasts of Vietnam and southern region, which could have arisen due to the mountain precipitation being resolved and not seen in the observations.

One of the ways to characterize climate variability and extremes is to calculate climate indices based on daily time series of basic variables such as precipitation and temperature, especially precipitation. This allows a first-cut assessment of

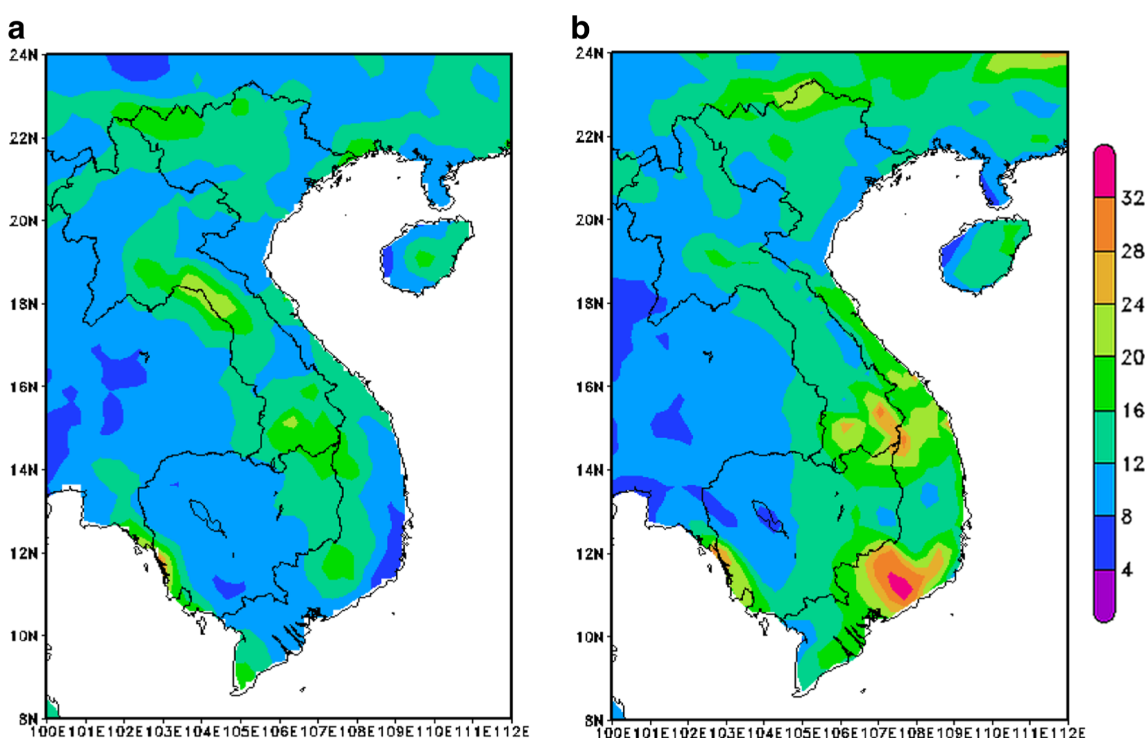

Fig. 11 Annual 90th percentile of daily rainfall, mm/day, 1961–1990. **a** APH, **b** WRF/ERA40

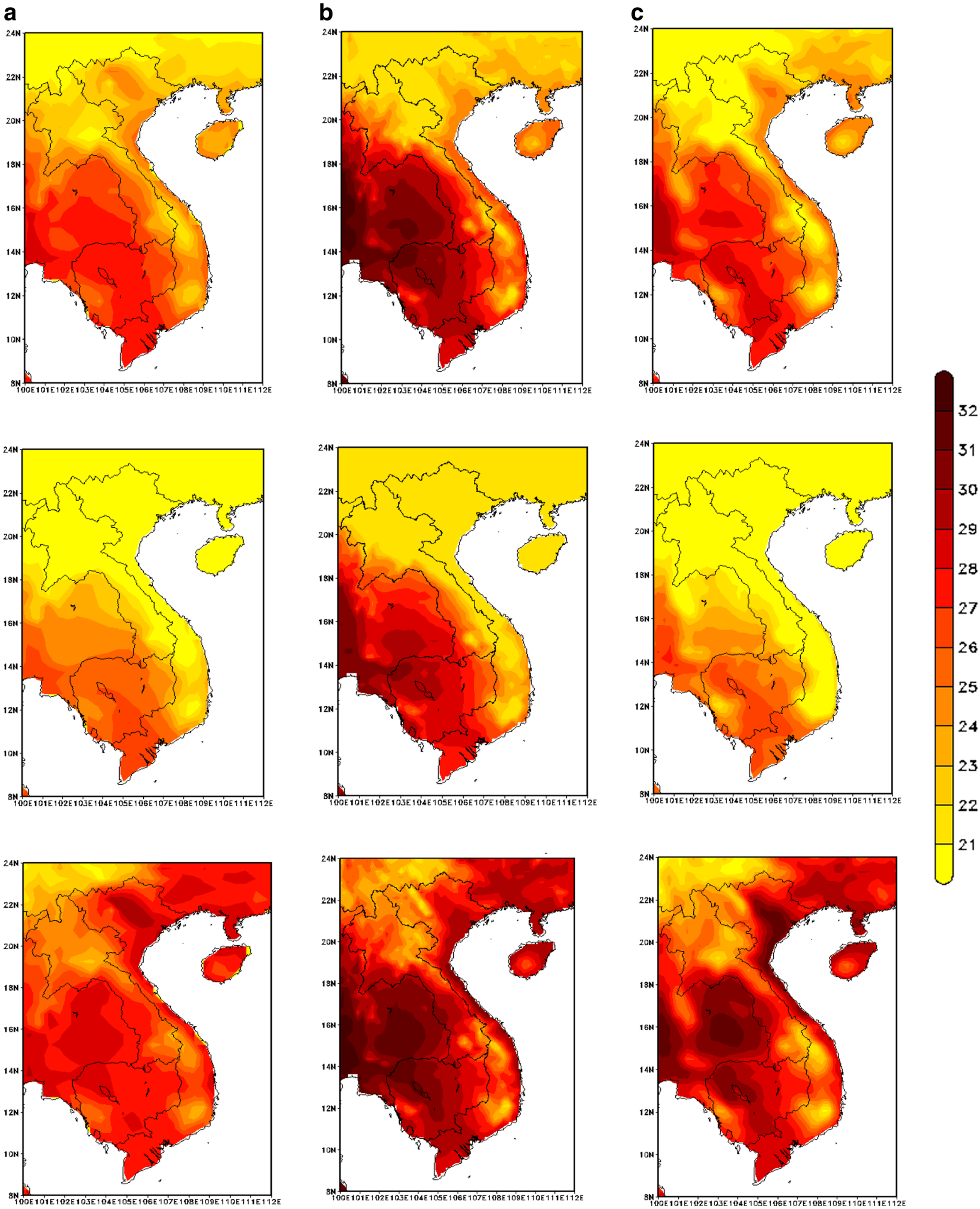

Fig. 12 Mean surface temperature, °C, 1961–1990. **a** CRU, **b** APH, **c** WRF/ERA40. Annual (*top*), DJF (*middle*), and JJA (*bottom*)

the capacity of the RCM driven in reanalyses mode to capture the main weather meteorological sequences, dealing with occurrence, duration, and intensity of precipitation events (i.e. percentage of number of wet days, mean intensity per

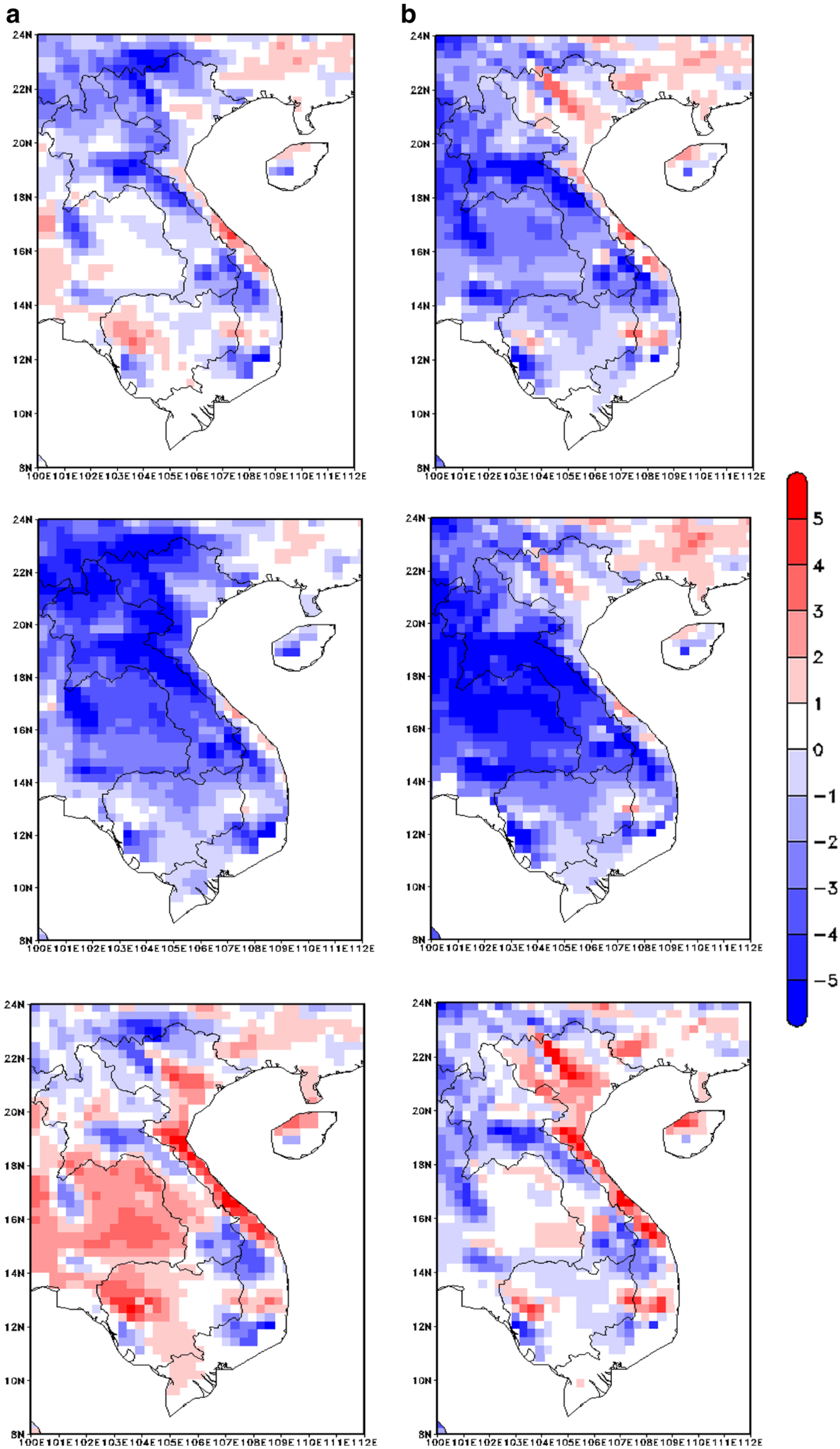

Fig. 13 Bias: WRF minus OBS mean surface air temperature, °C, 1961–1990. OBS: **a** CRU, (**b**) APH

wet day (referred to here as the simple daily intensity index) and the 90th percentile of daily rainfall. These indices are used by several international research groups who have recently developed a standard methodology for calculating such indices (see ETCCDMI—Expert Team on Climate Change Detection and Indices, http://cccma.seos.uvic.ca/ETCCDMI/index.shtml, the European research project known as STARDEX—Statistical and Regional dynamical Downscaling of Extremes for European regions, cited at: www.cru.uea.ac.uk/cru/projects/stardex). The WRF simulations are further validated further using the number of wet days, simple daily intensity index, and 90th percentile of rainfall, shown from Figs. 9, 10, and 11, respectively.

As far as the wet day frequencies are concerned, the WRF simulated rainfall shows better agreement with APHRODITE than with CRU. However, some differences between WRF and APHRODITE as to a higher (lower) variability over central highlands (Mekong Delta region) are apparent. The rain intensity (Fig. 10) indicates that WRF agrees largely with APHRODITE over Vietnam. The extreme 90th percentile of rainfall also shows better agreement against APHRODITE.

The temperature patterns are rather better simulated than precipitation. These are shown in Fig. 12. The annual and seasonal patterns of temperature distributions are better resolved when compared to the gridded observations. Nevertheless, some parts of northern Vietnam show warmer temperatures than the observations in JJA. The mean annual temperature biases, shown in Fig. 13 indicate that the WRF model is able to resolve temperature fields with least biases over most of the regions except in some central and northern parts of Vietnam. Some cold biases exist over some western boundaries and southern regions of Vietnam during the winter months, and some warm biases are seen during the summer months over central Vietnam. The areal averages over different regions also shows that the WRF model was able to better simulate the mean surface temperatures (Table 2).

The mean annual cycles for the temperature profiles are also shown in Fig. 14 for the three stations after a terrain height correction of the WRF model using the method of Sheridan et al. (2010). At Hanoi, the WRF model overestimates the mean monthly temperature values during the early months of the year until August. The model closely follows

Table 2 Areal average annual temperature for three main regions: North, Center, and South

Mean	North	Center	South
APHRO	20.8	24.1	27.8
CRU	22.7	24.6	27.2
WRF/ERA40	21.6	23.4	27.6

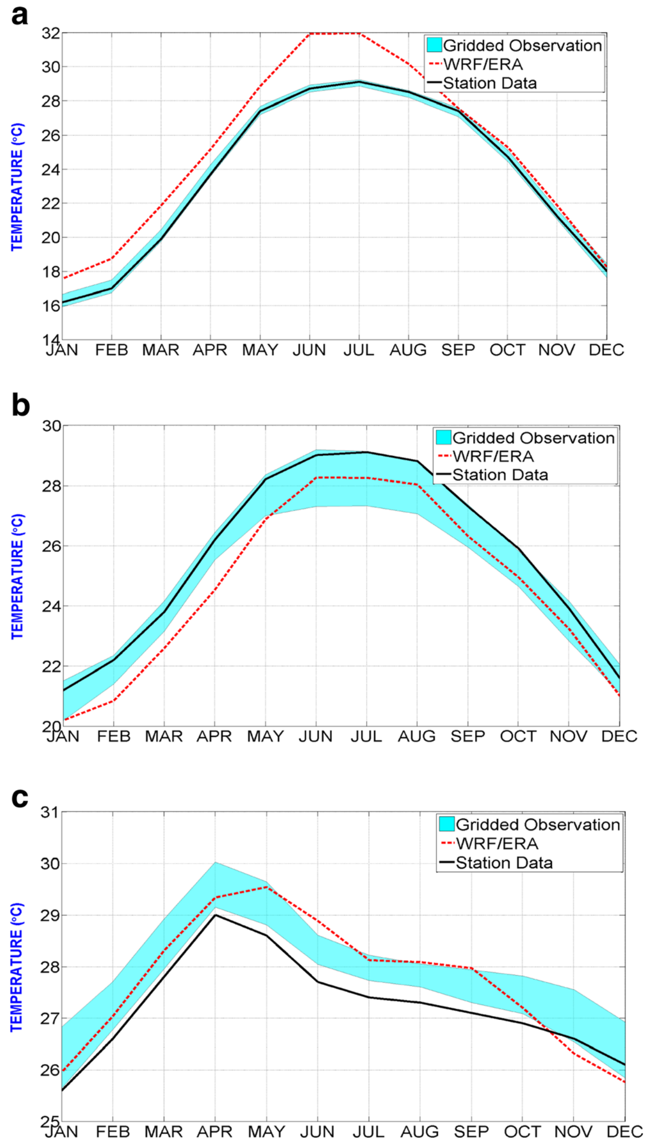

Fig. 14 Mean annual cycle of surface air temperature, °C, 1961–1990. **a** Hanoi, **b** Da Nang, **c** Ho Chi Minh City

the station data profiles at Da Nang and at Ho Chi Minh city, although with a cool bias at Da Nang and slightly higher values during some of the months at Ho Chi Minh city. The probability distributions of temperature (Fig. 15) over the three stations indicate a better agreement of the model to observations over Da Nang and Ho Chi Minh than over Hanoi.

Some statistical metrics have been shown in Table 3, for both precipitation and temperature, in support of further validation of the WRF model against the observations (Station data). The four metrics tabulated on annual averages for the correlation coefficient (CC), the mean absolute error (MAE), the root mean squared error (RMSE), and the actual bias values, at the three station locations of Hanoi, Da Nang, and Ho Chi Minh city. For precipitation, Da Nang shows the highest CC, MAE, and RMSE and the least bias of the three stations. Though the RMSE is the least for Hanoi, the CC is

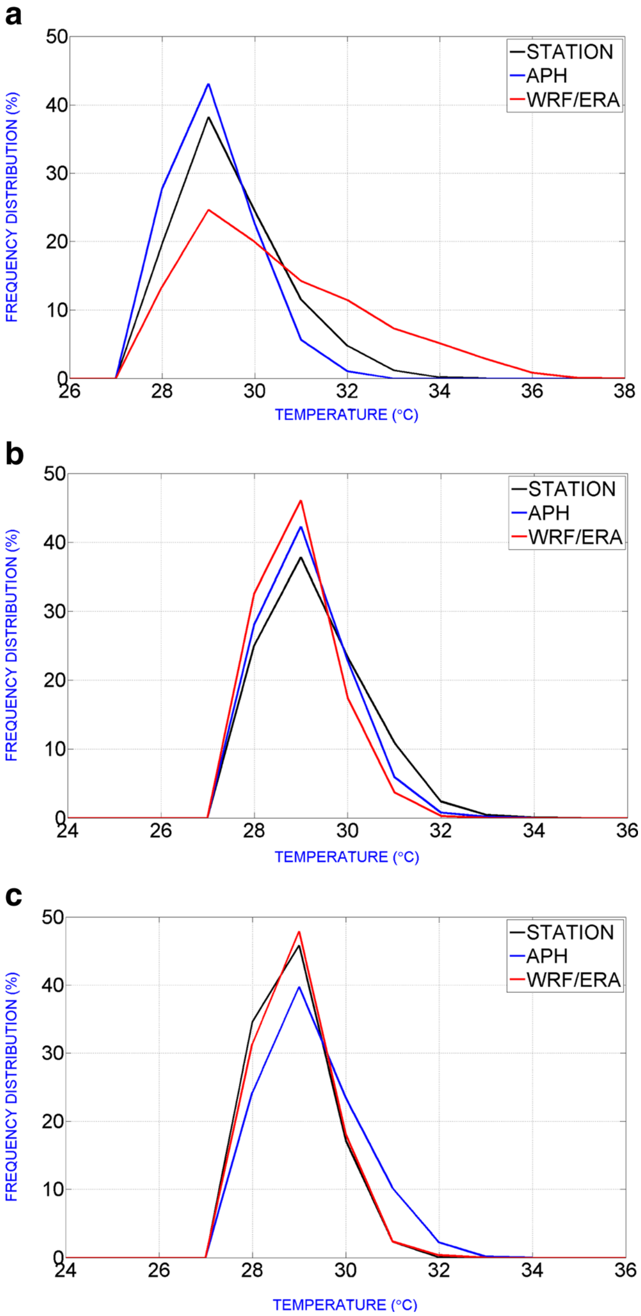

Fig. 15 Probability density function of temperature, °C, 1961–1990. **a** Hanoi, **b** Da Nang, **c** Ho Chi Minh City

also the lowest of all. For temperature, all stations exhibit high correlations above 0.8 °C; the biases are nearly ±1 °C. Hanoi shows the highest RMSE of all the stations. These results also indicate that while the model is able to reproduce some characteristics of the observed, it might not be possible to reproduce all the observed characteristics on all the locations. This also leads to test the limits of spatial resolutions as to what could be the best resolution that could show better results for all locations, given that finer scales do not necessarily mean best results. Along with the rest of the model behavior discussed earlier on, these metrics show yet another facet of the uncertainties in the models that need to be treated with caution when the results are applied for impact studies.

Table 3 Statistical metrics comparing WRF against station data (left) precipitation and (right) temperature

Metrics	WRF vs STA	Metrics	WRF vs STA
Hanoi		Hanoi	
CC	0.61	CC	0.89
MAE mm	2.53	MAE °C	1.97
RMSE mm	3.84	RMSE °C	2.63
Bias mm	(−)1.26	Bias °C	(+)0.95
Da Nang		Da Nang	
CC	0.76	CC	0.92
MAE mm	5.28	MAE °C	1.46
RMSE mm	7.74	RMSE °C	1.71
Bias mm	(+)0.58	Bias °C	(−)1.05
Ho Chi Minh City		Ho Chi Minh City	
CC	0.72	CC	0.81
MAE mm	2.94	MAE °C	0.87
RMSE mm	4.28	RMSE °C	1.91
Bias mm	(+)0.81	Bias °C	(+)0.99

Additional evaluations of wind profiles and rainfall predictors (sea level pressure and geopotential heights) are also useful to understand how well the regional climate model is able to reproduce the observed state of climate. In addition, these circulation features are also important as they are contributing factors to rainfall dynamics. We also present a bird's eye view of these features from Figs. 16, 17, 18, 19, and 20, compared on the two monsoon seasonal basis. In all these figures, the ERA40 reanalysis is kept as observational reference. The surface winds [zonal (u10) and meridional winds (v10) at 10 m] are shown in Fig. 16. The WRF model reproduces the regional circulation, and the wind flow during the two seasons (northeast; south-west) is captured well. The regional model also shows some strong wind flow over the southern coast of Vietnam during both seasons over the South China Sea. The WRF model resolves the DJF season of the upper winds at 850 mb better than during JJA, though the wind flow pattern is simulated well when compared to ERA40 reanalyses (Fig. 17). The upper winds at 200 mb are resolved well by the WRF model during both seasons (Fig. 18). Figures 19 and 20 show that the WRF model is able to reproduce the observed patterns of sea level pressure and geopotential heights during both seasons very well.

4 Summary and conclusions

Thirty-year (1961–1990) integrations of the WRF model driven by the ERA40 reanalyses were performed over

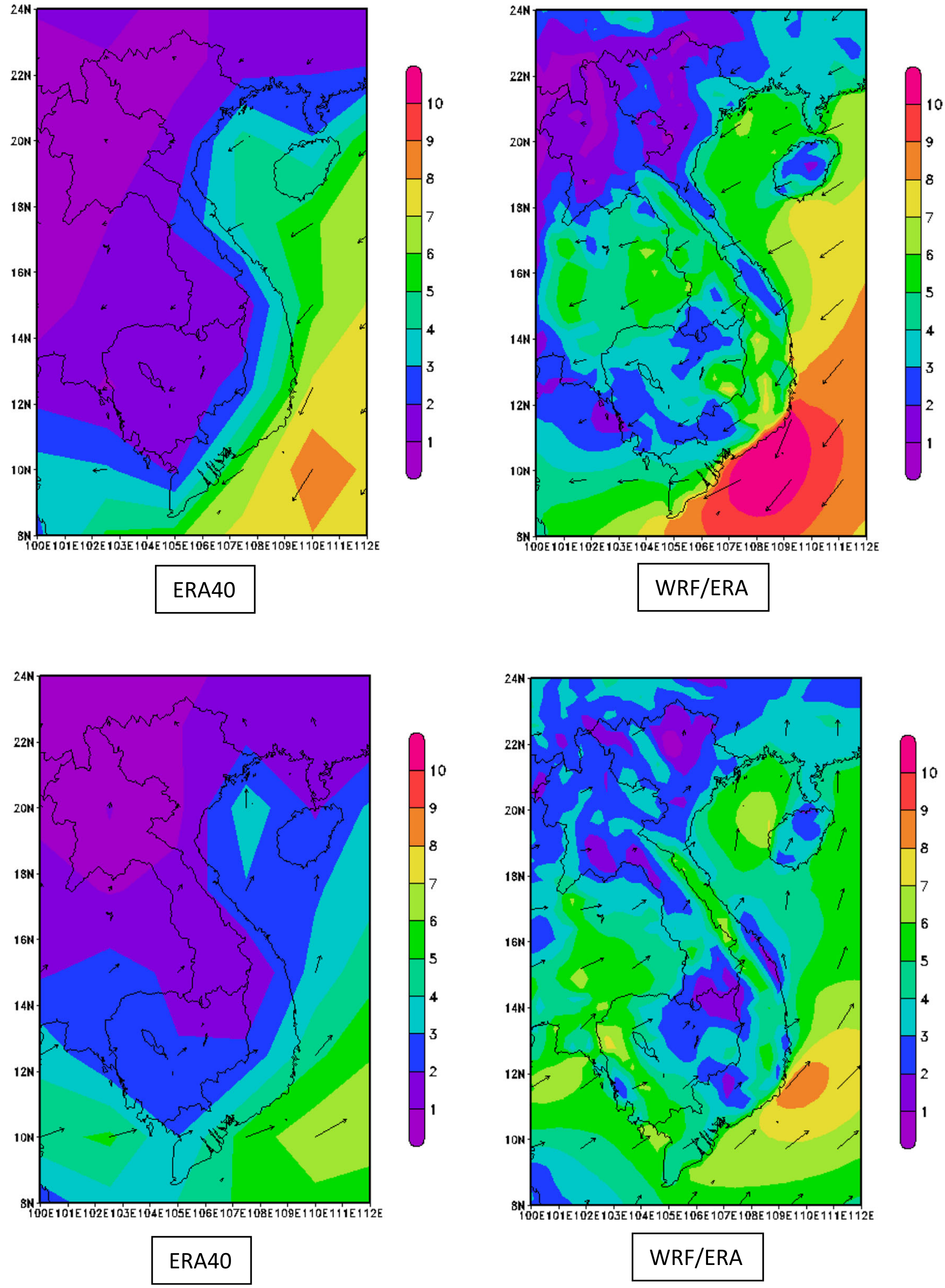

Fig. 16 Surface winds, m/s, 1961–1990 (*top*) DJF (*bottom*) JJA

Vietnam to assess the skill of the model in reproducing the mean state of climate over the present day. The results showed that the WRF model was able to better simulate the climate fields. Some differences exist among the different gridded observations themselves, but this range has been used to represent observational uncertainty.

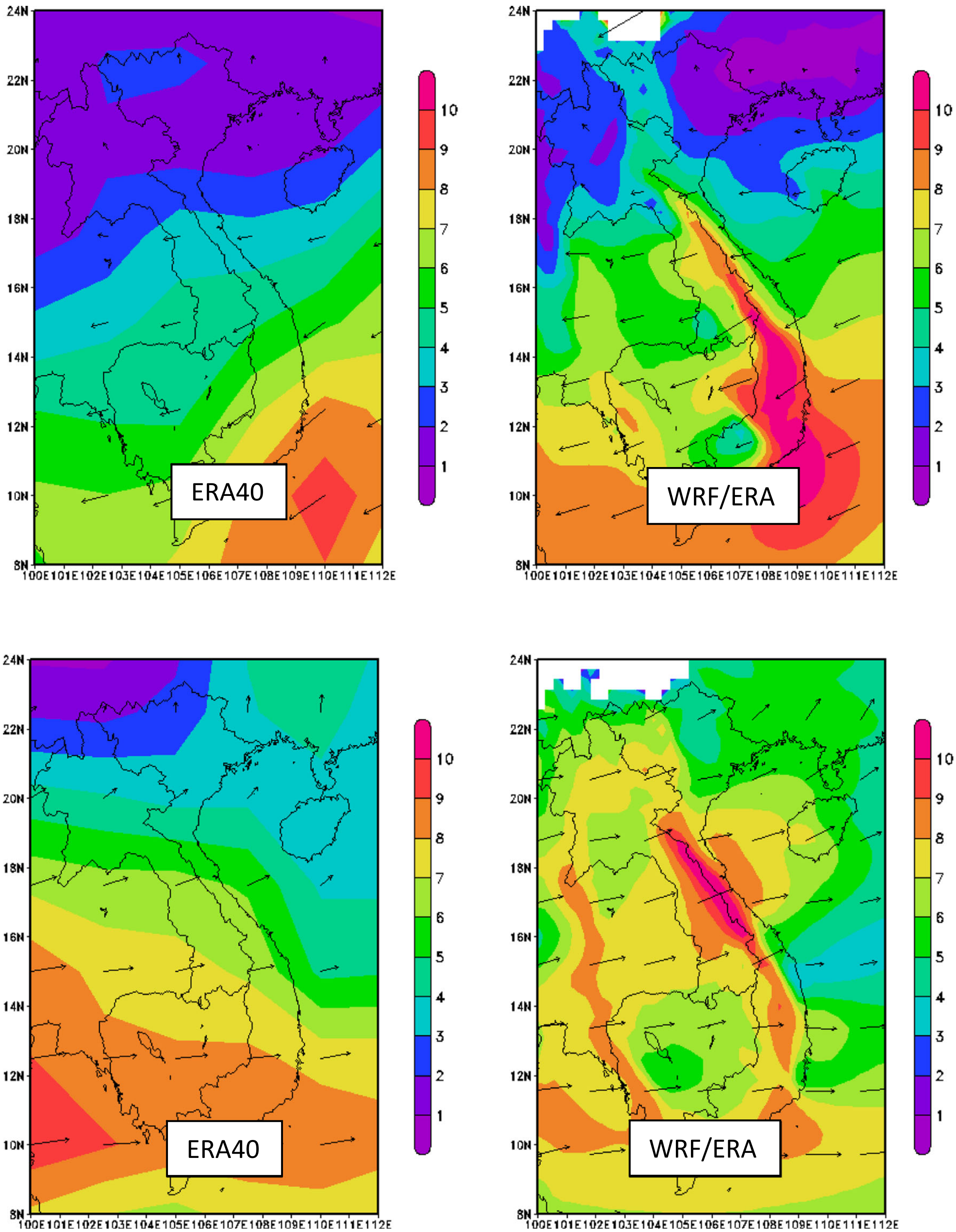

Fig. 17 Upper winds at 850 mb, m/s, 1961–1990 (*top*) DJF (*bottom*) JJA (*white* areas in WRF/ERA indicates terrain mask over the Tibetan plateau)

Quantifying those observational uncertainties is out of the scope of this paper, and they are merely used for bench marking model performance. The mean temperature fields are generally better simulated compared to precipitation (which is more variable in space and time). The model performed generally better on an annual scale, but, overall, some improvement in the model simulation during the summer months is necessary. The model was also able to capture the higher intensities of precipitation, although there is a general trend of underestimating dry days. The

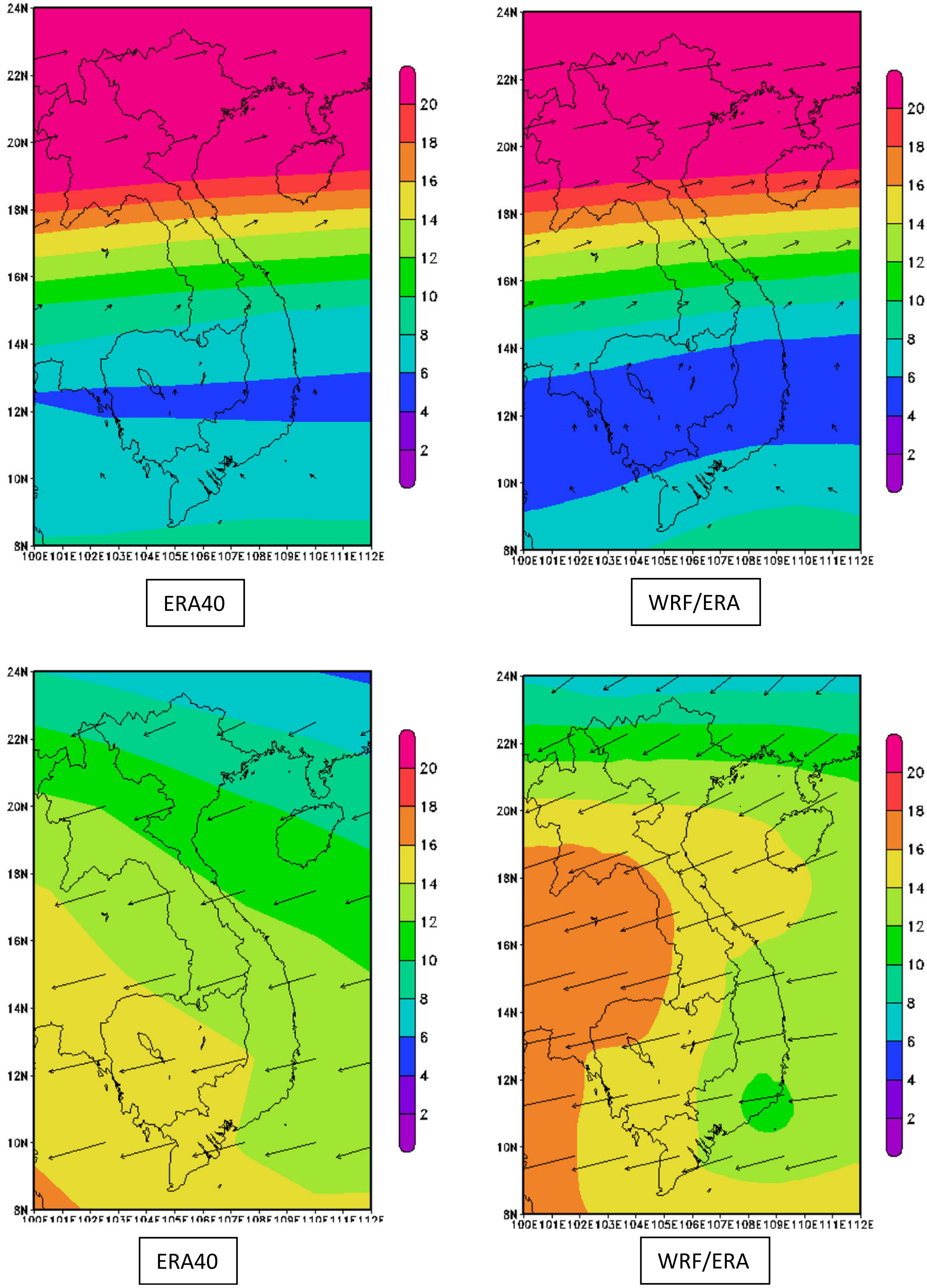

Fig. 18 Upper winds at 200 mb, m/s, 1961–1990 (*top*) DJF (*bottom*) JJA

model was able to better simulate interannual variability and the annual cycles of precipitation and temperature. The seasonal surface and upper winds and the patterns of observed sea level pressure and geopotential heights are

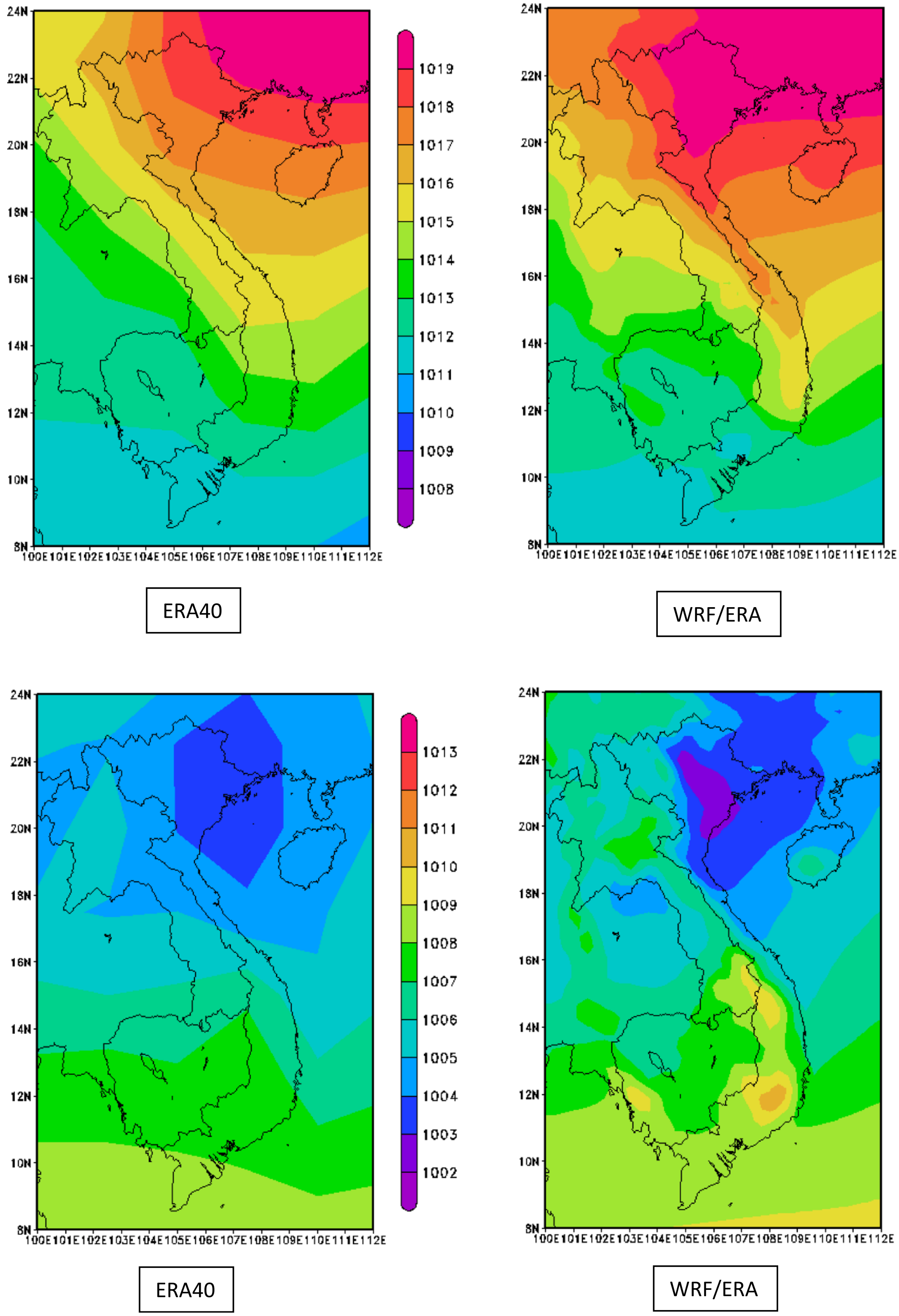

Fig. 19 Mean sea level pressure (mb), 1961–1990 (*top*) DJF (*bottom*) JJA

also well resolved by the model. Overall, the WRF model was able to better simulate the mean state of climate over Vietnam. However, as dynamical downscaling experiments have become common and are deemed robust for impacts application, the study suggests that at local scales and sub-regional scales, the accuracy still needs to be improved. As

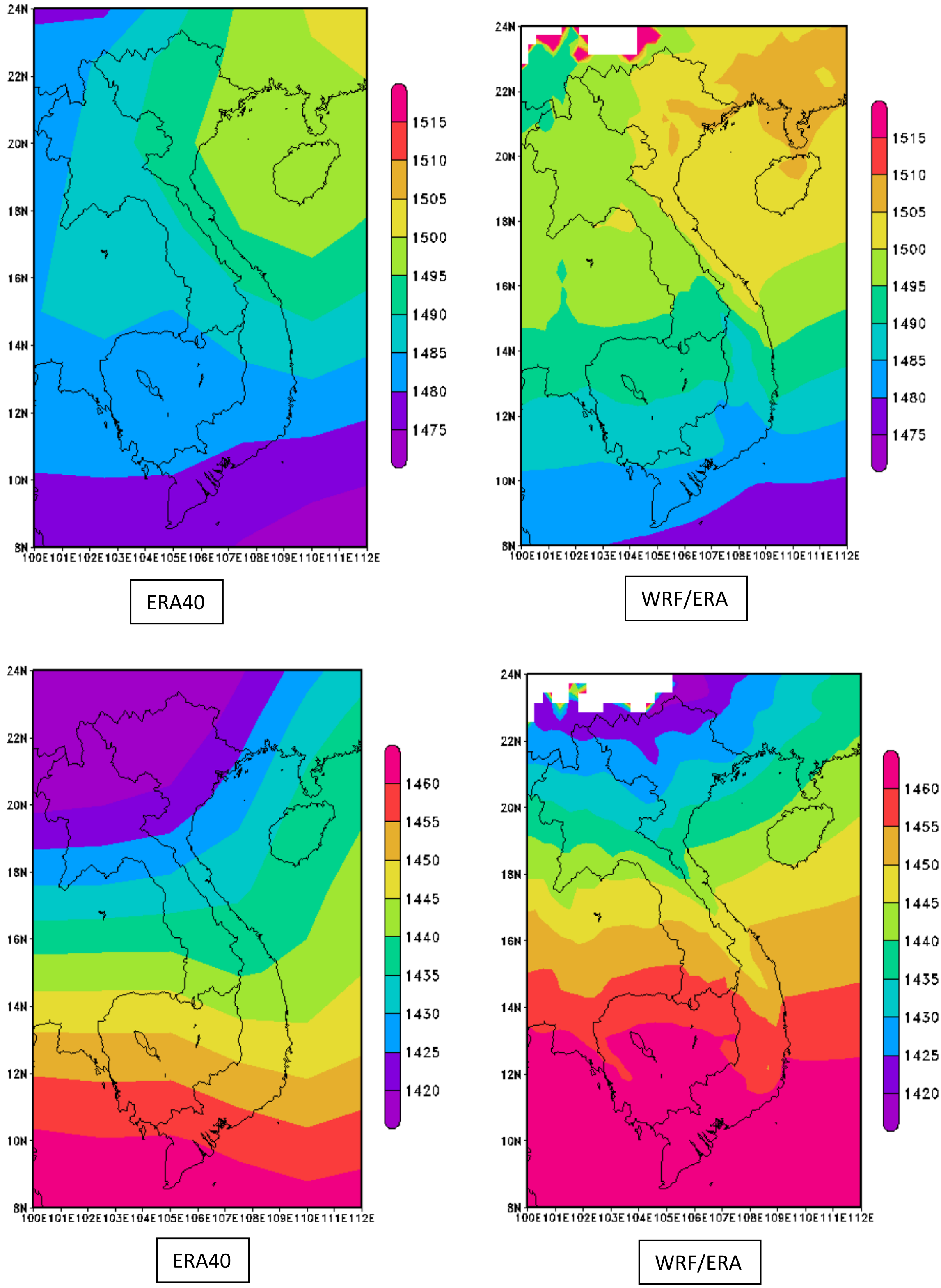

Fig. 20 Geopotential heights (m), 1961–1990 (*top*) DJF (*bottom*) JJA (*white* areas in WRF/ERA indicates terrain mask over the Tibetan plateau)

that lies with the modeling community, the study also adds impetus to the note that a dense network of observations is highly important when it comes to model evaluations. However, the study is a contribution to add to the very few dynamical downscaling studies that exist over this region. Future climate analyses are underway.

Acknowledgments The authors profusely thank the anonymous reviewers who have helped us to refine the contents of the manuscript that has improved the quality of the paper.

References

Chen F, Dudhia J (2001) Coupling an advanced land surface–hydrology model with the Penn State–NCAR MM5 modeling system. Part I: model implementation and sensitivity. Mon Weather Rev 129:569–585

Chotamonsak C, JP Salathe, J Kreasuwan, S Chantara and K Siriwitayakorn 2011. Projected climate change over Southeast Asia simulated using a WRF regional climate

Fowler HJ, Ekstrom M, Kilsby CG, Jones PD (2005a) New estimates of future changes in extreme rainfall across the UK using regional climate model integrations—assessment of control climate. J Hydrol 300(1–4):212–233

Frei A, Miller JA, Robinson DA (2003) Improved simulations of snow extent in the second phase of the Atmospheric Model Intercomparison Project (AMIP-2). J Geophys Res 108(D12): 4369. doi:10.1029/2002JD003030

Frei C, Scholl R, Fukutome S, Schmidli J, Vidale PL (2006) Future change of precipitation extremes in Europe: intercomparison of scenarios from regional climate models. J Geophys Res 111:D06105. doi:10.1029/2005JD005965

Giorgi F (1990) Simulations of regional climate using a limited area model nested in a general circulation model. J Clim 3(9):941–963

Grell GA (1993) Prognostic evaluation of assumptions used by cumulus parameterizations. Mon Weather Rev 121(3):764–787

Hewitson BC, Crane RG (2006) Consensus between GCM climate change projections with empirical downscaling: precipitation downscaling over South Africa. Int J Climatol 26(10):1315–1337

Hong SY, Pan HL (1996) Nonlocal boundary layer vertical diffusion in a medium-range forecast model. Mon Weather Rev 124(10):2322–2339

IPCC, 2007: Climate change 2007: the physical science basis. Contribution of working group I to the fourth assessment report of the intergovernmental panel on climate change. S Solomon, D Qin, M Manning, Z Chen, M Marquis, KB Averyt, M Tignor and HL Miller, (Eds.) Cambridge University Press, Cambridge, 996 pp

Leung LR, Qian Y, Bian X, Washington WM, Han J, Roads JO (2004) Mid-century ensemble regional climate change scenarios for the western United States. Clim Chang 62(1–3):75–113

Mitchell TD, Jones PD (2005) An improved method of constructing a database of monthly climate observations and associated high-resolution grids. Int J Climatol 25:693–712

New M, Hulme M, Jones PD (1999) Representing twentieth century space-time climate variability. Part 1: development of a 1961-90 mean monthly terrestrial climatology. J Clim 12:829–856

New M, Hulme M, Jones PD (2000) Representing twentieth century space-time climate variability. Part 2: development of 1901-96 monthly grids of terrestrial surface climate. J Clim 13:2217–2238

Phan VT, Thanh ND, Ho TMH (2009) Seasonal and interannual variations of surface climate elements over Vietnam. Clim Res 40:49–60

Schmidli J, Frei C, Vidale PL (2006) Downscaling from GCM precipitation: a benchmark for dynamical and statistical downscaling methods. Int J Climatol 26(5):679–689

Sheridan P, Smith S, Brown A, Vosper S (2010) A simple height-based correction for temperature downscaling in complex terrain. Meteorol Appl 17:329–339

Skamarock WC, Klemp JB, Dudhia J, Gill DO, Baker DM, Duda MG, Hwang XY, Wang W, Powers JG (2008) A description of the advanced research WRF version 3. Technical Note 475+STR. National Centre for Atmospheric Research, Boulder

Takahashi HG, Yoshikane T, Hara M, Yasunari T (2009) High resolution regional climate simulations of the long term decrease in September rainfall over Indochina. Atmos Sci Lett 10:4–18

Takahashi HG, Yoshikane T, Hara M, Yasunari T (2010) High resolution modelling of the impact of land surface conditions on regional climate over Indochina associated with the diurnal precipitation cycle. Int J Climatol 30(13):2004–2020

Thompson G, Rasmussen RM, Manning K (2004) Explicit forecasts of winter precipitation using an improve bulk microphysics scheme. Part-I: description and sensitivity analysis. Mon Weather Rev 132(2):519–542

Uppala SM et al (2005) The ERA40 reanalysis. Q J R Meteorol Soc 131(612):2961–3012

Wang Y et al. (2004) Regional climate modeling: progress, challenges and prospects. J Meteorol Soc Jpn 82:1599–1628

Yatagai A, Kamiguchi K, Arakawa O, Hamada A, Yasutomi N, Kitoh A (2012) APHRODITE: constructing a long-term daily gridded precipitation dataset for Asia based on a dense network of rain gauges. Bull Am Meteorol Soc. doi:10.1175/BAMS-D-11-00122.1